PAPER

Enhanced legume root growth with pre-soaking in α-Fe₂O₃ nanoparticle fertilizer†

Soubantika Palchoudhury, [iD] *[a] Katherine L. Jungjohann,[b] Lakmali Weerasena,[c] Abdollah Arabshahi,[d] Uday Gharge,[a] Abdulaziz Albattah,[a] Justin Miller,[a] Ketan Patel[a] and Robert A. Holler[e]

The rising demand for food and energy crops has triggered interest in the use of nanoparticles for agronomy. Specifically, iron oxide-based engineered nanoparticles are promising candidates for next-generation iron-deficiency fertilizers. We used iron oxide and hybrid Pt-decorated iron oxide nanoparticles, at low and high concentrations, and at varied pHs, to model seed pre-soaking solutions for investigation of their effect on embryonic root growth in legumes. This is an environmentally friendly approach, as it uses less fertilizer, therefore less nanoparticles in contact with the soil. Analysis from varied material characterization techniques combined with a statistical analysis method found that iron oxide nanoparticles could enhance root growth by 88–366% at low concentrations (5.54×10^{-3} mg L^{-1} Fe). Hybrid Pt-decorated iron oxide nanoparticles and a higher concentration of iron oxide nanoparticles (27.7 mg L^{-1} Fe) showed reduced root growth. The combined materials characterization and statistical analysis used here can be applied to address many environmental factors to finely tune the development of vital nanofertilizers for high efficiency food production.

1 Introduction

The expanding global population and rising use of bioenergy crops demand nearly a 70% increase in our current agricultural production by 2050, according to the Food and Agricultural Organization of the United Nations.[1] To meet this target with the current rural workforce, new and sustainable strategies will need to be developed such as high-efficiency fertilizers. Traditional chemical nutrients are absorbed at low efficiency by plants, though nanoparticles (NPs) can provide enhanced uptake and transport within the plants due to their small size and high surface area. The United States Department of Agriculture has recognized the importance of nanotechnology to increase agricultural production through its Agricultural Food and Research Initiative.[2,3]

Due to these improved transport mechanisms of NPs, researchers have begun investigating engineered nanostructures/nanoparticles (ENPs) for their potential use in next generation fertilizers.[4–6] Raju *et al.*, reported a significant increase in water uptake and enhanced germination of green gram seeds with 1 mM Fe NPs.[7] Srivastava *et al.*, used iron pyrite NPs to induce marked increase in growth rate of spinach plants.[8] In terms of transport, ENPs have been observed to penetrate tomato plant roots and seed tissues,[9] and more specifically, iron oxide NPs have demonstrated absorption into watermelon plants.[10] Iron oxide NPs are of particular interest for nanofertilizers, as they are more benign compared to Fe NPs and iron is required by the plants to generate chlorophyll for photosynthesis.[11] Recently, iron oxide NPs were used in replacement for commercial Fe-fertilizers to successfully replenish Fe deficiency in peanut plants.[5] As nanostructures can now be made in reproducible shapes, sizes, alloyed structures, core–shell structures, and surface functionalization; the most active NP structure for improved plant growth and root absorption is still an active area of research.[12–14]

The complexity in the NP concentration within the fertilizer is based on providing enough of the dense nutrient within the soil to benefit the plant growth, without over-loading the soil to cause decreased plant biomass, decreased root length, and possibly plant toxicity.[15–17] Limited reports are available on the interaction of plants with iron oxide based NPs,[18,19] though Zhu

[a]*Department of Civil and Chemical Engineering, University of Tennessee at Chattanooga, Chattanooga, Tennessee 37403, USA. E-mail: soubantika-palchoudhury@utc.edu; Fax: +1-423-425-5229; Tel: +1-423-425-5455*

[b]*Center for Integrated Nanotechnologies, Sandia National Laboratories, Albuquerque, New Mexico 87185, USA*

[c]*Department of Mathematics, University of Tennessee at Chattanooga, Chattanooga, Tennessee 37403, USA*

[d]*SimCenter and Department of Mechanical Engineering, University of Tennessee at Chattanooga, Chattanooga, Tennessee 37403, USA*

[e]*Central Analytical Facility, The University of Alabama, Tuscaloosa, Alabama 35487, USA*

† Electronic supplementary information (ESI) available: Experimental details: XEDS image of Pt-iron oxide NPs; XRD and FT-IR plots of iron oxide NPs; Table showing size of different seeds; Plots showing the growth rate of green pea, green gram, black bean, and red bean seedlings in iron oxide and hybrid NPs; images showing first and second generation legume plants in potted soil; SEM-XEDS image of green gram roots grown in low concentration of iron oxide NPs and high concentration of Pt-decorated iron oxide NPs; FT-IR plots of black bean roots grown in low and high concentration of iron oxide NP growth solution. See DOI: 10.1039/c8ra04680h

et al. demonstrated that 500 mg L^{-1} of iron oxide NPs did not exert any toxicological effect in pumpkin plants over a prolonged exposure period.[20] In addition, a study on green gram seeds showed that the 10 mg L^{-1} iron oxide NPs facilitated an increased physiological activity.[14] In a study on soybean plants, magnetite NPs of concentration 60 mg L^{-1} were seen to translocate within the plant and increase chlorophyll levels.[21] More recently, Jeyasubramanian *et al.*, reported higher growth rate of spinach plants with hematite NPs (100–200 mg Fe) in hydroponic conditions.[22] In this study, the slightly acidic pH of the hydroponics facilitated conversion of Fe^{3+} to water soluble Fe^{2+} ions, which were then absorbed by the plants. Therefore, iron oxide NPs present an optimal source for iron delivery to plants within fertilizers. However, the NP structure, concentration, and NP absorption have not been optimized.[23]

Soil pH is also a significant parameter in integrating ENPs as it largely influences the plant root's absorption of the nutrient.[24] The absorption of the NPs is dependent on the surface functionality, transformations in morphology, surface structure, and agglomeration state of the NPs after interaction with natural organic matter or nutrients in the environment, irrespective of the type of NP.[25,26] Typically, these mineral nutrients and biomolecules displace weaker binding surface ligands on the NP surface to form hybrid NPs, distinct from the original synthesized state of the ENP. Aggregation state of NPs also significantly affected nutrient absorption by plant roots.[27] However, most studies on plants have reported the interactions of as-synthesized iron oxide NPs without taking into account the effect of particle transformation or pH. We have developed hybrid Pt-decorated iron oxide NPs and growth solutions at different pHs to address this issue. No information is currently available in the literature of a comparative study between iron oxide and hybrid Pt–Fe$_2$O$_3$ nanostructures.

In this study, we have investigated an experimental matrix of beaker-type NP-containing aqueous growth solutions on edible legumes of different sizes (*e.g.*, green gram (mung bean), black bean, chickpea, green pea, and red bean) that represent a significant fraction of crops consumed world-wide (Fig. 1). Fifteen different growth solutions were tested over a period of six days for each of the five legume seeds with variances in NP type (functionalized iron oxide *vs.* Pt-decorated iron oxide), NP concentration (0.00554 mg L^{-1} and 27.7 mg L^{-1}), and solution pH (5.5, 7, and 8) as compared to growth solutions without NPs. This is the first report comparing the interaction of seeds with iron oxide NPs and a newly formulated Pt-decorated hybrid counterpart. Each experiment was repeated six times to obtain reliable growth rates. Root samples were characterized after the growth period using electron microscopy and Fourier-transform infrared spectroscopy (FTIR). We found that the low concentration (0.00554 mg L^{-1}) of iron oxide NPs enhanced root growth of all of the edible legumes by 88–366%, with the most significant growth rate observed for green gram seeds. These studies will be useful in developing a new class of Fe-enhanced fertilizers, and methods for pre-soaking seeds in nutrient dense solutions at the initial stages of germination for seamless nutrient absorption and decreased fertilizer quantity for enhanced environmental safety.

2 Methods

2.1 Materials

All reagents including iron(III) acetylacetonate (Fe(acac)$_3$, 99%, Alfa Aesar), polyvinylpyrrolidone (PVP, M_w 10 kDa, TCI, Fisher), polyethyleneimine (PEI, M_w 60 kDa, 50% aq., Alfa Aesar), triethyleneglycol (C$_6$H$_{14}$O$_4$, TREG, 99%, Acros), de-ionized water (DI, Fisher), hexachloroplatinic acid (H$_2$PtCl$_6$, 10%, 3.8% Pt, EMD Millipore), sodium hydroxide (NaOH, 97%, Fisher), and hydrochloric acid (HCl, 35%, Fisher) were used as purchased. Seeds of green pea (*Pisum sativum* L.), chick pea (*Cicer arientinum*), green gram or mung bean (*Vigna radiate*), black and red beans (*Phaseolus vulgaris*) were purchased from local grocery stores in Chattanooga, Tennessee, USA.

2.2 Synthesis of iron oxide nanoparticles

Iron oxide NPs were synthesized *via* a "modified" polyol method.[28] In a typical synthesis, a capping molecule mixture of

Fig. 1 Schematic overview of the experimental matrix used for seed root growth quantification. 15 growth solutions were studied for each of the five legume seeds over a 6 day period. In addition, the entire matrix was repeated six times for reliable statistical analysis.

PVP (0.7 g) and PEI (0.3 g) was heated to dissolution in solvent, TREG (10 mL) at 90 °C for 10 min. 2 mmol of the iron precursor, Fe(acac)$_3$ was added to this solution and mixed for 10 min. TREG also served as the reducing agent in the reaction. The reactant solution was then thermally decomposed at 260 °C for 1 h to form the final iron oxide NP product. The entire synthesis was conducted in air without any inert gas protection.

The NPs were cleaned *via* centrifugation (high-speed mini-centrifuge, Fisher Scientific) for 15 min at 14 000 rpm to remove any organics as the supernatant. The iron oxide NPs were dissolved in DI water and sonicated for 15 min (Branson 1800, room temperature) to obtain well-mixed final product at the desired concentration (*e.g.*, 5.54×10^{-3} and 27.7 mg L^{-1} Fe). The concentrations were confirmed using two methods; calculations based on sample weight and calibration plots obtained from ultraviolet-visible spectroscopy (UV-vis). These iron oxide NPs served as seeds for the synthesis of the Pt-decorated iron oxide NPs. In addition, the NPs were used in subsequent NP-seed interaction experiments.

2.3 Synthesis of Pt-decorated iron oxide nanoparticles as hybrid nanoparticle sample

Hybrid NPs contain two or more different components attached or integrated within the NP unit. Here, Pt-attached iron oxide NPs were synthesized as model hybrid NPs following a previously published protocol.[29] Typically, aqueous solution of the Pt precursor (H$_2$PtCl$_6$) was mixed with iron oxide NPs at 10 : 1 Pt precursor : NP volume ratio. The Pt precursor was subsequently reduced to Pt NPs on iron oxide surfaces using 30 min ultraviolet (UV) irradiation with a hand-held UV lamp (Fisher). The UV-reduction time was kept at 30 min to control the size of Pt NPs on iron oxide surfaces. Identical to the iron oxide NPs, these NPs were also cleaned *via* centrifugation and dissolved in DI water *via* sonication to obtain target mass concentrations of 5.54×10^{-3} and 27.7 mg L^{-1} Fe.

2.4 Measuring the growth of roots in seeds soaked in nanoparticles

Effect of iron oxide and Pt-decorated iron oxide NPs on different seeds (*e.g.*, green pea or *Pisum sativum* L., chick pea or *Cicer arientinum*, green gram or *Vigna radiate*, black beans, and red beans or *Phaseolus vulgaris*) was assessed specifically in terms of root growth in a span of six days. Seeds were cleaned in 75% ethanol and DI water and thoroughly dried with filter paper prior to exposure to growth solution. In addition, vials used for these experiments were sterilized in 70% ethanol. Samples of the same seed type were placed in three growth solutions: control DI water solution, a solution representing lower NP concentration (5.54×10^{-3} mg L^{-1} Fe), and a higher concentration of NP solution (27.7 mg L^{-1} Fe). The seeds were taken out of the solution for measurement each day and the root length was measured using Vernier calipers for up to six days. It should be noted that green gram roots, being soft, required careful handling for measurement with Vernier calipers. The experiments were conducted at room temperature under ambient pressure conditions. For each seed type, this

experiment was repeated six times with both iron oxide and Pt-iron oxide NPs for statistical analysis.

The root growth experiment described above was conducted in different pH solutions (*e.g.*, pH 5.5, 7, and 8) for each seed type to investigate any pH-dependent changes in NP-embryonic root interaction.

2.5 Characterization of the nanoparticles and roots

The size and morphology of the iron oxide and Pt-decorated iron oxide NPs were investigated on a FEI Tecnai F-20 transmission electron microscope (TEM). The iron oxide NPs were measured to be ∼16 nm in size (Fig. 2A) and the Pt NPs to be ∼2 nm (Fig. 2B). Pt-decoration was observed to be irregular over the iron oxide NPs though attachment of Pt NPs on iron oxide seeds was indicated by XEDS data (Fig. S1, ESI†). The hydrodynamic diameter and zeta potential of iron oxide and hybrid Pt-decorated iron oxide NPs were measured on a Litesizer 500 Particle Analyzer (Anton Paar). The hydrodynamic diameter of aqueous iron oxide NP solution was 118 nm with a polydispersity index of 0.17, indicating good uniformity in size (Fig. 2C). In comparison, the hydrodynamic size of Pt-iron oxide NPs was lower (86 nm, polydispersity index: 0.12) due to the presence of small sized Pt NPs and the complex morphology of these NPs (Fig. 2D). Both iron oxide NPs and Pt-decorated iron oxide NPs showed a negative surface charge, though the low absolute value of zeta potential indicated steric stabilization of these NP surfaces (Fig. 2E and F). The crystal structure of
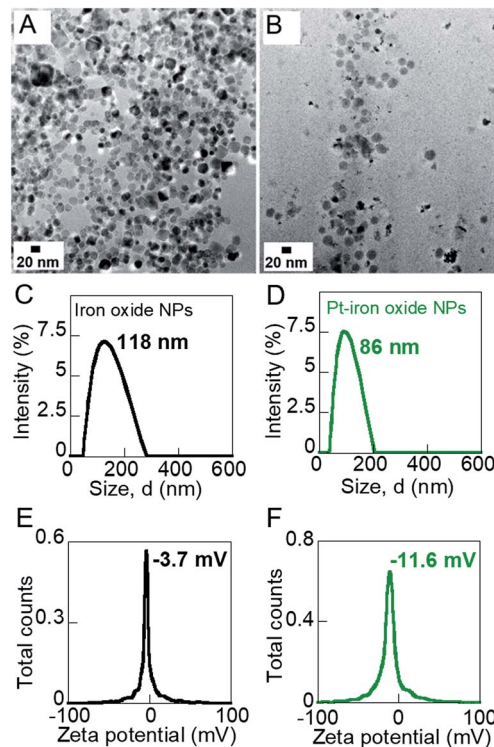

Fig. 2 Characterization of iron oxide and hybrid Pt-decorated iron oxide NPs. (A) TEM image, iron oxide NPs, (B) TEM image, Pt-iron oxide NPs, (C) hydrodynamic diameter plot, iron oxide NPs, (D) hydrodynamic diameter plot, Pt-iron oxide NPs, (E) zeta potential plot, iron oxide NPs, and (F) zeta potential plot, Pt-iron oxide NPs.

powdered NP samples was investigated on a Philips Analytical X-ray diffractometer (XRD) equipped with a Cu source. Fig. S2, ESI† shows the powdered XRD measurement of the NPs to confirm their crystal phase. The peaks of iron oxide NPs matched well with hematite (α-Fe_2O_3) crystal structure.

A multi-method material characterization technique was used to understand the effect of the nanofertilizers on the embryonic legume roots. Both the morphology and chemical composition of the roots were characterized using a FEI Titan ChemiSTEM (Thermo Scientific) with high-collection-angle X-ray energy dispersive spectroscopy (XEDS). A JEOL 7000 FE scanning electron microscope (SEM) equipped with XEDS was used to identify the overall surface and chemical composition of the roots. To characterize the surface functional groups on the roots, a Bruker Alpha Fourier transform infrared spectrometer (FT-IR) was used over 400–4000 cm^{-1} range on well-dried root samples. The FT-IR data was used to investigate the differences between the various NP growth solutions on embryonic root growth by detecting the surface ligands on the roots.

3 Results and discussion

The control DI water (0 mg L^{-1} Fe), low (5.54×10^{-3} mg L^{-1} Fe), and high concentration (27.7 mg L^{-1} Fe) growth solutions were prepared with iron oxide NP and hybrid Pt-decorated iron oxide NPs, respectively, for each seed type (seed sizes varied with type, as shown in Table S1, ESI†) to investigate dose-dependent response of the seedlings. Both iron oxide and hybrid Pt-decorated iron oxide NPs showed notable effect on the development of embryonic roots. However, a significant increase in root length was observed in low concentration iron oxide NP solutions for chick peas (88%), green peas (160%), and green gram (366%) in comparison to the control solutions. The most notable enhancement of root growth was seen in green gram and chick pea seeds, likely due to their requirement for iron. Fig. 3A and B show images of the embryonic roots for the green

gram seeds soaked in iron oxide and hybrid Pt-decorated iron oxide NP solutions, respectively. In general, the Pt-decorated iron oxide solutions produced root growth for all seed types, though not as great in comparison to the iron oxide NP solutions under equivalent conditions.

Results from our root growth study over a six-day period are represented in detailed statistical plots for both iron oxide and hybrid Pt-decorated iron oxide NPs for each of the five seed types. The statistical results conveyed two findings; iron oxide NPs facilitated better root growth as compared to the hybrid Pt-decorated iron oxide NPs and the low concentration iron oxide growth solution proved to be the best soak solution for increased root growth. Specifically, Fig. 4A and B showed time-dependent plots of the average root length of chickpea seeds in iron oxide and hybrid NPs, respectively. The control, low, and high NP concentrations were marked as water, low NP, and high NP, respectively in the plots for both iron oxide and hybrid NPs (Fig. 4). At low concentrations $\sim 5.54 \times 10^{-3}$ mg L^{-1} Fe, iron oxide NPs significantly enhanced root growth, as suggested from the time-dependent root length plot in Fig. 4A. Though an inhibitory effect was observed at high NP concentrations ($\sim$27.7 mg L^{-1} Fe), roots were seen in all tested samples for iron oxide NPs (Fig. S3, ESI†). The hybrid Pt-decorated iron oxide NPs exhibited a reduced growth rate of the roots as compared to the iron oxide NPs, but did not completely inhibit development of embryonic roots (Fig. 4B and S4, ESI†). The fact that the different legume seeds showed higher root growth in iron oxide NP growth solution in comparison to the hybrid Pt-decorated iron oxide NPs or the control DI water growth solutions was also supported through comprehensive statistical analysis using two-factors repeated measures analysis of variance (ANOVA) computed in MATLAB (Table S2, ESI†). Since iron oxide NP growth solutions performed better than Pt-decorated
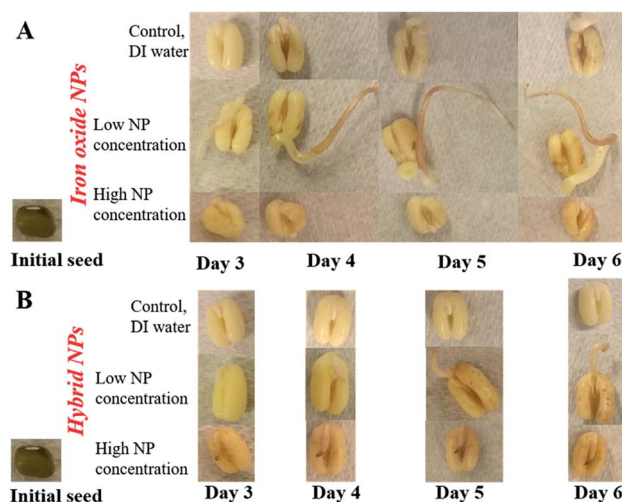

Fig. 3 Seedling growth with NP fertilizer at pH 7. (A) Green gram root grown in iron oxide NP solution and (B) green gram root growth in hybrid Pt-decorated iron oxide NPs. Low NP concentration was 5.54×10^{-3} mg L^{-1} Fe, and high was 27.7 mg L^{-1} Fe.
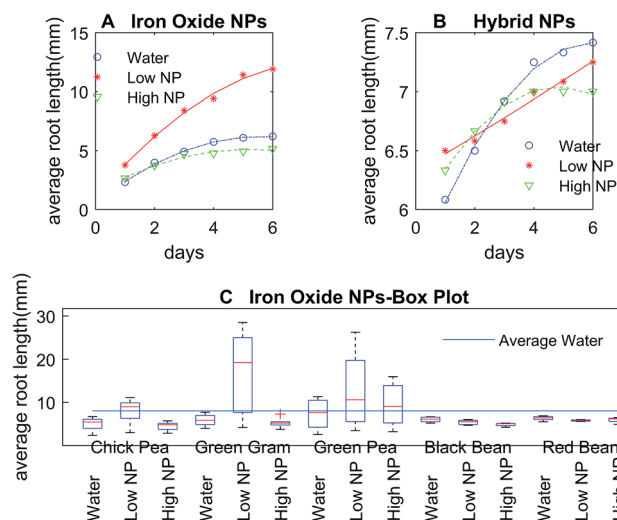

Fig. 4 Time-dependent NP-seed interaction plots. (A) Iron oxide NP-chick pea, (B) hybrid Pt-decorated iron oxide NP-chick pea, and (C) iron oxide NP-different seeds at pH 7; 95% confidence interval used; the average root length for all water grown seeds is indicated (average water) in the box plot as a benchmark for comparison. Low NP concentration was 5.54×10^{-3} mg L^{-1} Fe, and high was 27.7 mg L^{-1} Fe.

iron oxide NPs, we investigated the comparative influence of iron oxide NPs at both low and high concentrations on the five different legumes in one representative statistical plot. Fig. 4C shows the box plots for average root length after six days for each seed type under different concentrations of iron oxide NP growth solutions at pH 7. When we compared these parameters for chickpeas, we observed that there was a significant increase in growth rate of the roots when using low NP concentrations in comparison to water (88% increase) and high NP (184% increase). Further, we observed that low iron oxide NP treatment enhanced the growth of green pea and green gram by 160% and 366%, respectively (Fig. 4C) in comparison to the control growth solution.

The effect of NPs depended on the size and type of seeds, in addition to the concentration and morphology of the NPs, based on these plots in Fig. 4. In comparison to chick pea, green pea, and green gram, the growth of black and red bean seedlings was not affected by ENPs (Fig. 4C, S3 and S4, ESI†). Embryonic roots were observed in all treated black and red bean seeds, but the growth rate of these roots was not enhanced by iron oxide NP fertilizer, unlike the other legume seeds tested. This was likely because these bean types are richer in iron content as compared to the other legume seeds. Therefore, they were less affected by Fe-deficiency fertilizers like iron oxide NPs as the average inherent iron concentration in beans (55 μg g^{-1}) is high in comparison to the other crops.[30]

In comparison of NP solutions at different pH conditions (pH 5.5, 7, and 8), the representative data from chick peas under the three growth solutions of control, low, and high iron oxide NP concentrations is shown (Fig. 5A and B). The embryonic roots showed the same dose response trend at all pHs, but a slower growth rate of embryonic roots was observed at pH 5.5 or 8 as compared to the neutral pH (Fig. 5A and B). Alternately, the NP concentration-growth trend of seedlings in hybrid Pt-

decorated NPs were more sensitive to pH (Fig. 5C and D), but embryonic roots were seen in all samples, suggesting absence of severe toxic effect of these NPs at concentrations < 27.7 mg L^{-1} Fe. Fig. S5 and S6 (ESI†) show successful growth of first generation legume plants in potted soil, grown from seeds pre-soaked in both low and high concentration of iron oxide NP solution (pH 7). We also demonstrated the healthy growth of one whole generation of chick pea plant from seeds soaked in low concentration iron oxide NPs of pH 7 (Fig. S5, ESI†). These plant growth experiments in potted soil rule out the possibility of adverse effect of iron oxide NP fertilizer, particularly at the low concentration.

The root surfaces were characterized via SEM and XEDS after a six-day growth period to investigate the changes in physiology and chemical composition after interaction with the NPs (Fig. 6). Fig. 6A shows the SEM image of embryonic green gram roots grown in DI water after Au sputtering. Intact epidermis was observed in the control sample grown in DI water. The epidermis was undamaged in roots grown in low concentration of iron oxide NPs, as suggested by the SEM image (Fig. 6B). In addition, these roots had prominent root hairs to facilitate increased absorption of nutrients, as shown by Fig. 6C. In contrast, discernable change in morphology of the epidermis was seen in embryonic roots grown in higher concentration of iron oxide NPs, suggesting possible adverse impact at these high NP concentrations (Fig. 6C and D).[31] Roots grown in Pt-iron oxide hybrid NPs showed NP aggregates on the surface, which likely caused the reduced growth of roots in these growth solutions (Fig. 6E). XEDS imaging confirmed the presence of Fe and O in roots grown in high concentration iron oxide NPs (Fig. S7, ESI†).

However, in roots grown in low concentration iron oxide NPs, the Fe was likely taken up or assimilated by the roots, as suggested by the absence of Fe in the XEDS image (Fig. S8, ESI†).[9] Interestingly, Fe and O were detected in roots grown in high concentration hybrid Pt-decorated NPs, but Pt was not seen on the root surface. One explanation for the absence of Pt in the XEDS plot would be not high enough sensitivity from the detector at this scale, or the possible selective absorption of the 2 nm Pt NPs through pores in the plant walls, which could consequently induce the slower root growth (Fig. S9, ESI†).[31]

On the other hand, iron oxide NP soak solutions, particularly at the low concentration induced fertilizer-like impact on legume seeds, based on our observations of different seedlings. Therefore, green gram roots grown in low and high concentration of iron oxide NPs for six days were characterized via TEM as representative samples to understand the role and the uptake of these NPs (Fig. 7). Sections of the roots were viewed directly without staining to clearly locate the NPs within the roots, without hindrance in contrast from the stain. The red arrows indicate probable aggregates of iron oxide NPs and individual NPs within the root sections. Roots grown in low concentration of iron oxide NPs did not show distinct particles in the images (Fig. 7A) as compared to the roots grown in high NP concentrations (Fig. 7B and insert). Regions of many NPs indicate the large number of NPs within the root structure for the high NP concentration sample. The root samples were further

Fig. 5 pH dependent NP–seed interaction plots for chick pea. (A) Iron oxide NPs, pH 5.5, (B) iron oxide NPs, pH 8, (C) hybrid NPs, pH 5.5, and (D) hybrid NPs, pH 8. Low NP concentration was 5.54 × 10^{-3} mg L^{-1} Fe, and high was 27.7 mg L^{-1} Fe.

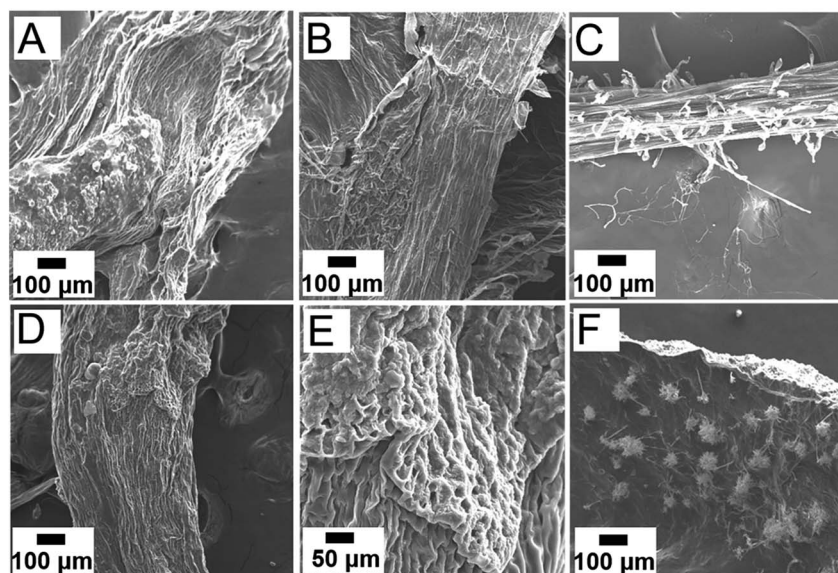**Fig. 6** SEM images of green gram roots grown in different growth solutions. (A) Control, DI water, (B) iron oxide NPs, low concentration (5.54 × 10^{-3} mg L^{-1} Fe), (C) section of sample B showing root hair, (D) iron oxide NPs, high concentration (27.7 mg L^{-1} Fe), (E) section of sample D showing morphological changes, and (F) high concentration of Pt-decorated iron oxide NPs.

characterized *via* XEDS and FT-IR spectroscopy to investigate the composition of particles absorbed and accumulated within the roots and a plausible mechanism to account for the increased root growth with iron oxide NP growth solution. A representative XEDS plot showing chemical composition of a section of green gram root grown in high concentration iron oxide NP pre-soak solution indicated presence of Fe and O, in addition to the C, P, S, Ca, and K from the organic components within the plant cells. This suggested absorption and accumulation of iron oxide NPs within the plant roots, based on the morphological information from TEM and SEM and the chemical composition from XEDS. Increased length in root hairs was also observed in legume seeds pre-soaked with low concentration iron oxide NP solution, which could account for increased nutrient uptake and the faster growth.[32]

To further understand why the iron oxide NPs caused increased growth of roots at low concentrations, we investigated the changes in chemical composition of embryonic roots

interacted with NPs. In specific, the surface functional groups of well-dried root samples after six-day growth were analyzed using FT-IR spectroscopy. A plausible chemical basis for interaction of the iron oxide nanofertilizer is suggested based on the FT-IR analyses. Fig. 8 shows the comparative FT-IR analysis of iron oxide NPs and green gram roots from seeds pre-soaked in different growth solutions. The FT-IR spectrum of hematite NPs used as the growth solution showed peaks in the fingerprint region at 520 cm^{-1} characteristic to the Fe–O stretching vibrations and 438 cm^{-1} corresponding to hydrogen bonds formed by OH groups adsorbed on the iron oxide surface.[22,33] The remaining peaks for hematite NPs characterize the PVP and PEI ligand coating on the NP surface. The peak at 1730 cm^{-1} was due to the C=O stretch from PVP ligand coating while the two adjacent peaks between 2380 cm^{-1} and 2300 cm^{-1} could be attributed to C–N triple bonds likely from the interaction of the two ligands, PVP and PEI.[34] The FT-IR spectrum of roots grown in low concentration iron oxide NPs exhibited the characteristic

Fig. 7 Scanning TEM images of embryonic green gram roots, grown in different concentrations of iron oxide NPs (A) low (5.54 × 10^{-3} mg L^{-1} Fe), (B) high (27.7 mg L^{-1} Fe), and (C) sample XEDS plot of B. Arrows and insert images show probable NP aggregates (A) and individual NPs (B) within root sections.
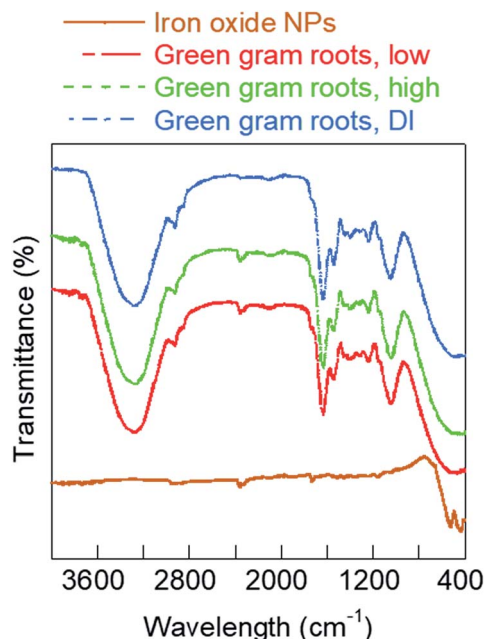
Fig. 8 FT-IR plots of iron oxide NPs and embryonic roots of green gram seeds grown in different concentrations of iron oxide NPs at neutral pH.

peaks at 2357 cm^{-1} and 2338 cm^{-1}, similar to that of PVP/PEI-coated iron oxide NPs (Fig. 8), indicating absorption of NPs by the roots. The other peaks of the spectrum were characteristic of root samples. Broadly, these included peaks at 3272 cm^{-1} due to O–H and N–H groups, 2927 cm^{-1} and 2855 cm^{-1} attributed to CH$_3$ and CH$_2$ stretching vibrations, 1635 cm^{-1} owing to amide I, 1542 cm^{-1} from lignin, 1396 cm^{-1} due to cellulose, 1238 cm^{-1} owing to carbonyl stretch in ester and amide III, and 1038 cm^{-1} characteristic to polysaccharides.[35,36] The FT-IR spectrum of green gram roots soaked in high concentration iron oxide NPs was similar to low concentration roots, indicating NP absorption by these root as well. However, the lignin content relative to that of polysaccharides and cellulose in these roots as indicated by the 1542/1038 cm^{-1} and 1542/1396 cm^{-1} peak ratios was different from the roots grown in low concentration iron oxide NPs.[37] This difference in lignin content and increased root hair account for the enhanced growth of legumes in low iron oxide NP pre-soak solutions as compared to the high concentration NPs. The peaks at 2357 cm^{-1} and 2338 cm^{-1} were absent in FT-IR spectrum of green gram roots grown in DI water, confirming our suggested mechanism of internalization of iron oxide NPs by the roots. Similar trends in FT-IR spectrum was also observed with black bean root samples grown in different pre-soak solutions (Fig. S10, ESI†). Detailed characterization of NP transport is currently being investigated through computational modeling.

4   Conclusions

In conclusion, a facile method was developed using different material characterization to assess the impact of two different iron oxide based nanostructures on root growth. The concentration, morphology, and chemical composition of the NPs and the type of seed were found to be major influences on the growth of embryonic roots, based on the results from five widely consumed legume seeds. The best growth in seedlings was observed with iron oxide NPs at low concentrations (∼5.54 × 10^{-3} mg L^{-1} Fe), though no effect was observed for black beans and red beans. The study served to prove that iron oxide NPs can improve growth rate of embryonic roots by 88–366% in some legume plants. The electron microscopy and FT-IR analysis of the roots confirmed NP absorption and provided key insights into dose-dependent changes in NP binding to the roots after exposure.

In this study, increased plant growth was achieved through pre-soaking the seeds in growth solutions. This was a more environment-friendly approach as it decreased the quantity of fertilizer used and eliminated the need for adding fertilizer to the soil. This study is impactful in two ways; first it reports a new iron oxide NP fertilizer and pre-soak method effective in increasing plant growth, and secondly, the combined material characterization and statistical method provides a novel approach to assess the efficiency of ENPs as nanofertilizers. Since the increase in plant growth with iron oxide NPs was observed for many seed types, it reliably predicts the great potential of iron oxide NPs as nanofertilizers.
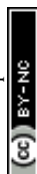
This integrated statistical and material characterization approach could serve as a new multi-method assessment metric for the application of iron oxide NPs in agriculture. The method will also be attractive in developing new nanofertilizer materials to enhance agricultural production, while minimizing the NP contamination impact on the soil environment.[38] A plausible mechanism was suggested for absorption of iron oxide NP fertilizer and enhanced root growth, based on the FT-IR data. However, further investigation of plant growth in soil will be required to understand growth trends and interaction with NP fertilizers on a wider species of plants. In addition, detailed mechanism of NP absorption and distribution within the plant will be essential in developing new iron oxide NP based fertilizers and is currently under investigation. Currently, studies are being conducted on chemical analysis, hyperspectral imaging, and TEM analysis of the root, shoot, and leaf samples from plants grown with NP soaked seeds to achieve this goal. Computational modeling on the transport of NPs within the roots is also being conducted.

Conflicts of interest

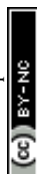There are no conflicts to declare.

Acknowledgements

performed, in part, at the Center for Integrated Nanotechnologies, an Office of Science User Facility operated for the U.S. Department of Energy (DOE) Office of Science. Sandia National Laboratories is a multi-mission laboratory managed and operated by National Technology and Engineering Solutions of Sandia, LLC., a wholly owned subsidiary of Honeywell International, Inc., for the U.S. DOE's National Nuclear Security Administration under contract DE-NA-0003525. The views expressed in the article do not necessarily represent the views of the U.S. DOE or the United States Government. The authors acknowledge Dr Jonathan Mies for use of XRD and Dr Manuel F. Santiago for use of FTIR. We thank UA CAF for use of SEM.

Notes and references

1 United Nations Food and Agricultural Organization. in *How to feed the world in 2050, Proceeding of an Expert Meeting on How to Feed the World in 2050*, FAO Headquarters, Rome, 2009.

2 R. Liu and R. Lal, Potentials of engineered nanoparticles as fertilizers for increasing agronomic productions, *Sci. Total Environ.*, 2015, **514**, 131–139.

3 X. Li, Y. Yang, B. Gao and M. Zhang, Stimulation of peanut seedling development and growth by zero-valent iron nanoparticles at low concentrations, *PLoS One*, 2015, **10**, e0122884.

4 N. Kottegoda, C. Sandaruwan, G. Priyadarshana, A. Siriwardhana, U. Rathnayake, D. Arachchige, A. Kumarasinghe, D. Dahanayake, V. Karunaratne and G. Amaratunga, Urea-hydroxyapatite nanohybrids for slow release of nitrogen, *ACS Nano*, 2017, **11**, 1214–1221.

5 M. Rui, C. Ma, Y. Hao, J. Guo, Y. Rui, X. Tang, Q. Zhao, X. Fan, Z. Zhang, T. Hou and S. Zhu, Iron oxide nanoparticles as a potential iron fertilizer for peanut (*Arachis hypogaea*), *Front. Plant Sci.*, 2016, **7**, 815.

6 A. Gogos, K. Knauer and T. D. Bucheli, Nanomaterials in plant protection and fertilization: current state, foreseen applications, and research priorities, *J. Agric. Food Chem.*, 2012, **60**, 9781–9792.

7 D. Raju, U. J. Mehta and S. R. Beedu, Biogenic green synthesis of monodispersed gum kondagogu (Cochlospermum gossypium) iron nanocomposite material and its application in germination and growth of mung bean (Vigna radiata) as a plant model, *IET Nanobiotechnol.*, 2016, **10**, 141–146.

8 G. Srivastava, C. K. Das, A. Das, S. K. Singh, M. Roy, H. Kim, N. Sethy, A. Kumar, R. K. Sharma, D. Philip and M. Das, Seed treatment with iron pyrite (FeS_2) nanoparticles increases the production of spinach, *RSC Adv.*, 2014, **4**, 58495–58504.

9 K. Shankramma, S. Yallappa, M. Shivanna and J. Manjanna, Fe_2O_3 magnetic nanoparticles to enhance *S. lycopersicum* (tomato) plant growth and their biomineralization, *Appl. Nanosci.*, 2016, **6**, 983–990.

10 J. Li, P. Chang, J. Huang, Y. Wang, H. Yuan and H. Ren, Physiological effects of magnetic iron oxide nanoparticles towards watermelon, *J. Nanosci. Nanotechnol.*, 2013, **13**, 5561–5567.

11 D. Alidoust and A. Isoda, Effect of gamma Fe_2O_3 nanoparticles on photosynthetic characteristic of soybean (Glycine max (L.) Merr.): foliar spray *versus* soil amendment, *Acta Physiol. Plant.*, 2013, **35**, 3365–3375.

12 J. Li, J. Hu, C. Ma, Y. Wang, C. Wu, J. Huang and B. Xing, Uptake, translocation and physiological effects of magnetic iron oxide (gamma-Fe_2O_3) nanoparticles in corn (*Zea mays* L.), *Chemosphere*, 2016, **159**, 326–334.

13 M. Vance, T. Kuiken, E. Vejerano, S. McGinnis, M. Hochella, D. Rejeski and M. Hull, Nanotechnology in the real world: redeveloping the nanomaterial consumer products inventory, *Beilstein J. Nanotechnol.*, 2015, **6**, 1769–1780.

14 H. Ren, L. Liu, C. Liu, S. He, J. Huang, J. Li, Y. Zhang, X. Huang and N. Gu, Physiological investigation of magnetic iron oxide nanoparticles towards chinese mung bean, *J. Biomed. Nanotechnol.*, 2011, **7**, 677–684.

15 L. Yin, B. Colman, B. McGill, J. Wright and E. Bernhardt, Effects of silver nanoparticle exposure on germination and early growth of eleven wetland plants, *PLoS One*, 2012, **7**, e47674.

16 C. Burklew, J. Ashlock, W. Winfrey and B. Zhang, Effects of aluminum oxide nanoparticles on the growth, development, and microRNA expression of tobacco (*Nicotiana tabacum*), *PLoS One*, 2012, **7**, e34783.

17 C. Rico, S. Majumdar, M. Duarte-Gardea, J. Peralta-Videa and J. Gardea-Torresdey, Interaction of nanoparticles with edible plants and their possible implications in the food chain, *J. Agric. Food Chem.*, 2011, **59**, 3485–3498.

18 Y. Feng, X. Cui, S. He, G. Dong, M. Chen, J. Wang and X. Lin, The role of metal nanoparticles in influencing Arbuscular Mycorrhizal fungi effects on plant growth, *Environ. Sci. Technol.*, 2013, **47**, 9496–9504.

19 K. S. Siddiqi and A. Husen, Plant response to engineered metal oxide nanoparticles, *Nanoscale Res. Lett.*, 2017, **12**, 92.

20 H. Zhu, J. Han, J. Xiao and Y. Jin, Uptake, translocation, and accumulation of manufactured iron oxide nanoparticles by pumpkin plants, *J. Environ. Monit.*, 2008, **10**, 713–717.

21 M. Ghafariyan, M. Malakouti, M. Dadpour, P. Stroeve and M. Mahmoudi, Effects of magnetite nanoparticles on soybean chlorophyll, *Environ. Sci. Technol.*, 2013, **47**, 10645–10652.

22 K. Jeyasubramanian, U. Thoppey, G. Hikku, N. Selvakumar, A. Subramania and K. Krishnamoorthy, Enhancement in growth rate and productivity of spinach grown in hydroponics with iron oxide nanoparticles, *RSC Adv.*, 2016, **6**, 15451–15459.

23 Y. Ma, L. Kuang, X. He, W. Bai, Y. Ding, Z. Zhang, Y. Zhao and Z. Chai, Effects of rare earth oxide nanoparticles on root elongation of plants, *Chemosphere*, 2010, **78**, 273–279.

24 N. K. Fageria and F. J. P. Zimmermann, Influence of pH on growth and nutrient uptake by crop species in an Oxisol, *Commun. Soil Sci. Plant Anal.*, 1998, **29**, 2675–2682.

25 A. Hitchman, G. Smith, Y. Ju-Nam, M. Sterling and J. R. Lead, The effect of environmentally relevant conditions on PVP stabilised gold nanoparticles, *Chemosphere*, 2013, **90**, 410–416.

26 M. Tejamaya, I. Roemer, R. C. Merrifield and J. R. Lead, Stability of citrate, PVP, and PEG coated silver nanoparticles in ecotoxicology media, *Environ. Sci. Technol.*, 2012, **46**, 7011–7017.

27 D. Martinez-Fernandez and M. Komarek, Comparative effects of nanoscale zero-valent iron (nZVI) and Fe_2O_3 nanoparticles on root hydraulic conductivity of *Solanum lycopersicum* L, *Environ. Exp. Bot.*, 2016, **131**, 128–136.

28 S. Palchoudhury and J. R. Lead, A facile and cost-effective method for separation of oil–water mixtures using polymer-coated iron oxide nanoparticles, *Environ. Sci. Technol.*, 2014, **48**, 14558–14563.

29 S. Palchoudhury, Y. Xu, J. Goodwin and Y. Bao, Synthesis of multiple platinum-attached iron oxide nanoparticles, *J. Mater. Chem.*, 2011, **21**, 3966–3970.

30 N. Petry, E. Boy, J. Wirth and R. Hurrell, Review: the potential of the common bean (*Phaseolus vulgaris*) as a vehicle for iron biofortification, *Nutrients*, 2015, **7**, 1144–1173.

31 M. Wang, L. Chen, S. Chen and Y. Ma, Alleviation of cadmium-induced root growth inhibition in crop seedlings by nanoparticles, *Ecotoxicol. Environ. Saf.*, 2012, **79**, 48–54.

32 K. Zygalakis, G. Kirk, D. Jones, M. Wissuwa and T. Roose, A dual porosity model of nutrient uptake by root hairs, *New Phytol.*, 2011, **192**, 676–688.

33 J. Fang, S. Li, W. Gong, Z. Sun and H. Yang, FTIR study of adsorption of PCP on hematite surface, *Spectrosc. Spectral Anal.*, 2009, **29**, 318–321.

34 S. Louie, J. Gorham, J. Tan and V. Hackley, Ultraviolet photo-oxidation of polyvinylpyrrolidone (PVP) coatings on gold nanoparticles, *Environ. Sci.: Nano*, 2017, **4**, 1866–1875.

35 P. Lagant, G. Vergoten, G. Fleury and M. Loucheuxlefebvre, Raman-spectroscopy and normal vibrations of peptides - characteristic normal-modes of a type-II beta-turn, *Eur. J. Biochem.*, 1984, **139**, 137–148.

36 A. Ertani, O. Francioso, E. Ferrari, M. Schiavon and S. Nardi, Spectroscopic-chemical fingerprint and biostimulant activity of a protein-based product in solid form, *Molecules*, 2018, **23**, 1031.

37 N. Ma, Y. Wang, S. Qiu, Z. Kang, S. Che, G. Wang and J. Huang, Overexpression of OsEXPA8, a root-specific gene, improves rice growth and root system architecture by facilitating cell extension, *PLoS One*, 2013, **8**, e75997.

38 R. Raliya, V. Saharan, C. Dimkpa and P. Biswas, Nanofertilizer for precision and sustainable agriculture: current state and future perspectives, *J. Agric. Food Chem.*, 2017, DOI: 10.1021/acs.jafc.7b02178.